Electronic Supplementary Material(ESI) for ChemComm.
This journal is © The Royal Society of Chemistry 2021

Supporting Information

Highly efficient catalytic oxidation of 5-hydroxymethylfurfural into 2,5-furandicarboxylic acid with bimetallic Pt-Cu alloy nanoparticles catalyst

Xiaomeng Cheng,[ab] Shaopeng Li,[c] Shulin Liu,[ab] Yu Xin,[ab] Junjuan Yang,[a] Bingfeng Chen*[a], and Huizhen Liu*[ab]

[a] Beijing National Laboratory for Molecular Sciences, CAS Key Laboratory of Colloid and Interface and Thermodynamics Institute of Chemistry, Chinese Academy of Sciences, Beijing 100190, P. R. China. E-mail: chenbf@iccas.ac.cn, liuhz@iccas.ac.cn

[b] University of Chinese Academy of Sciences, Beijing 100149, P. R. China

[c] Tianjin Key Laboratory of Molecular Optoelectronic Sciences, Department of Chemistry, Institute of Molecular Aggregation Science, Tianjin University, Tianjin 300072, P. R. China.

Table of Contents:

1.Experimental section

Materials

Activated charcoal(AC) and $H_2PtCl_6 \cdot 6H_2O$ were obtained from Acros Organic. $CuCl_2$ was obtained from Alfa Aesar China Co., Ltd. HMF(98%), FDCA(97%), FFCA(98%), DFF(98%) and HMFCA(98%) were obtained from J&K Scientific Ltd. $NaBH_4$ was obtained from Guangdong Guanghua Sci-Tech Co., Ltd. High-purity oxygen was obtained from Beijing Jinghui gas Sci-Tech Co., Ltd. All the chemical reagents were used as received without any further purification. In the process of preparing the catalyst, deionized water was used.

Synthesis of Pt-Cu/AC

500 mg of activated charcoal were suspended in 50 mL water. After stirring for 1 h, the appropriate amount of H_2PtCl_6 and $CuCl_2$ solution was added dropwise into AC dispersion under stirring. Then aqueous solution containing fresh $NaBH_4$ was added drop-wise with a continuous magnetic stirring, the reaction solution was kept on stirring for 2 h to complete the reduction reaction. The obtained granules were collected by centrifuging, washed with ultrapure water (3×30 mL) and ethanol (2× 30 mL) and dried in a vacuum oven at 60^{o}C for 12 h.

Oxidation reaction

The HMF oxidation reaction was carried out in a Teflon-lined stainless-steel reactor. In a typical experiment, 0.3mmol HMF, catalyst and solvent were packed into the reactor. The reactor was purged with pure oxygen twice to remove the air and finally boosted to 1MPa. Then the temperature was increased to 150 °C at 600 rpm. After 6 h, the reactor was placed in ice bath and the gas was released. The liquid reaction mixture was centrifuged and filtered. The quantitative analysis of the liquid products was conducted using HPLC equipment. The HPLC analysis was conducted on a Shimadzu Prominence liquid chromatograph (LC-20TA) equipped with a C18 column (XBridge, 4.6 mm × 150 mm× 3.5 μm particle size, Waters Corporation) and an UV-Vis detector (SPD-20A). Mobile phase A is 0.1% formic acid aqueous solution adjusted to pH ~ 3 with ammonium formate and mobile phase B was acetonitrile. The flow rate is 0.4 mL min^{-1}. The quantification of HMF and its oxidation products was performed based on the calibration curves of those standard compounds purchased from commercial vendors. The external standard method was used as the quantitative method of conversion of HMF and yield of FDCA, FFCA and DFF.

$$HMF\ Conversion\ (\%) = \frac{mol\ of\ HMF\ consumed}{mol\ of\ initial\ HMF} \times 100\%$$

$$Yield\ (\%) = \frac{mol\ of\ product\ formed}{mol\ of\ initial\ HMF} \times 100\%$$

Characterization

The transmission electron microscopy (TEM) images were obtained using JEOL-2100F and JEOL-F200 high-resolution transmission electron microscopes (HR-TEM) equipped with EDX. Powder X-ray diffraction (XRD) patterns were collected using a X-ray diffractometer (Model D/MAX2500, Rigaka) with Cu-Kα radiation. X-ray photoelectron

spectroscopy (XPS) analysis was performed on a Thermo Scientific ESCA Lab 250Xi using 200 W monochromatic Al Kα radiation, and a 500 µm X-ray spot was used. The base pressure in the analysis chamber was about 3×10^{-10} m bar. Typically, the hydrocarbon C 1s line at 284.8 eV from adventitious carbon was used for energy referencing. The metal contents of the catalysts were determined by using a Perkin Elmer Optima 2000 OV inductively coupled plasma-optical emission spectroscopy (ICP-OES).

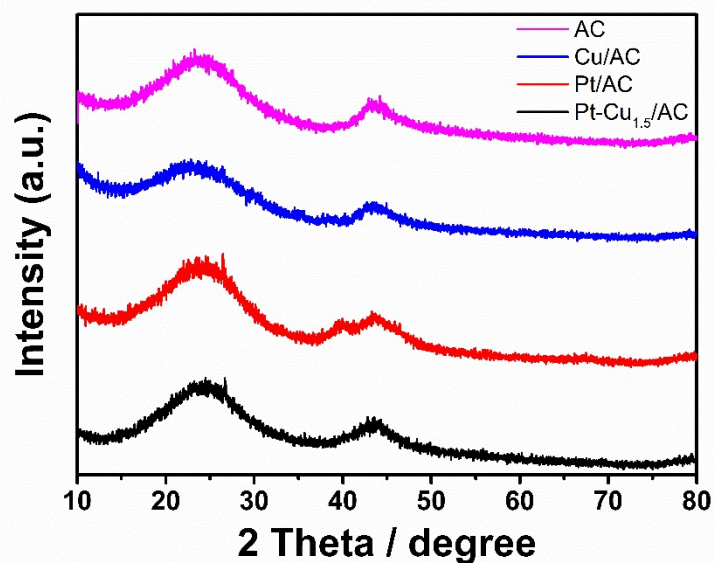

Figure S1. XRD patterns of Pt-$Cu_{1.5}$/AC, Cu/AC, Pt/AC and pure activated charcoal.

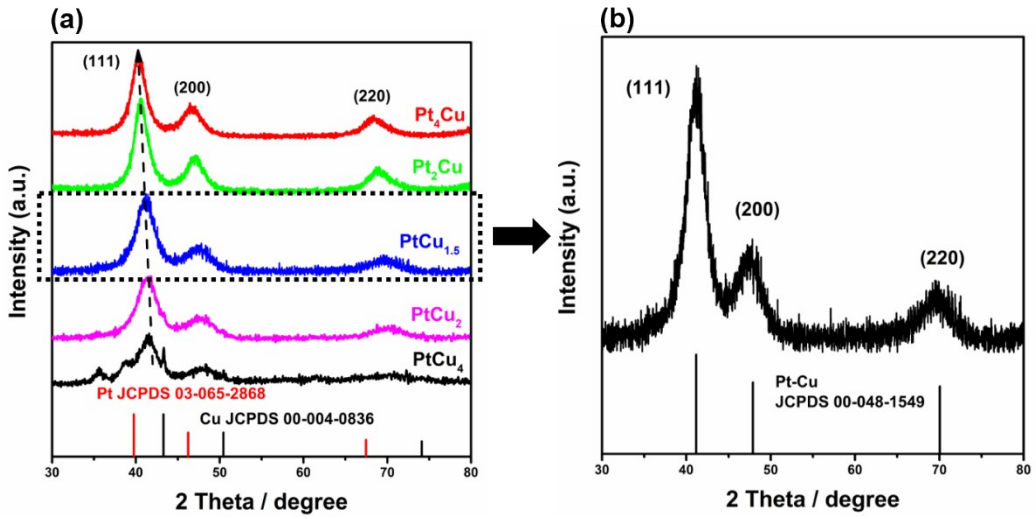

Figure S2. XRD patterns of (a) different ratios of Pt-Cu bimetallic nanoparticles and standard patterns of Pt and Cu cubic phase; and (b) Pt-$Cu_{1.5}$ nanoparticles with standard Pt-Cu alloy pattern.

To further investigate the synergistic effects of the Pt-Cu nanoparticles, the Pt-Cu bimetallic nanoparticles were prepared by the similar method in the absence of the carbon supports, and the related XRD patterns were displayed in Figure S2. The peaks in the Pt-Cu pattern shifted slightly to a higher angle, locating between Cu (JCPDS No.00-004-0836) and Pt (JCPDS No. 03-065-2868), indicating the reduction of structural lattice parameter due to the formation of the alloy.

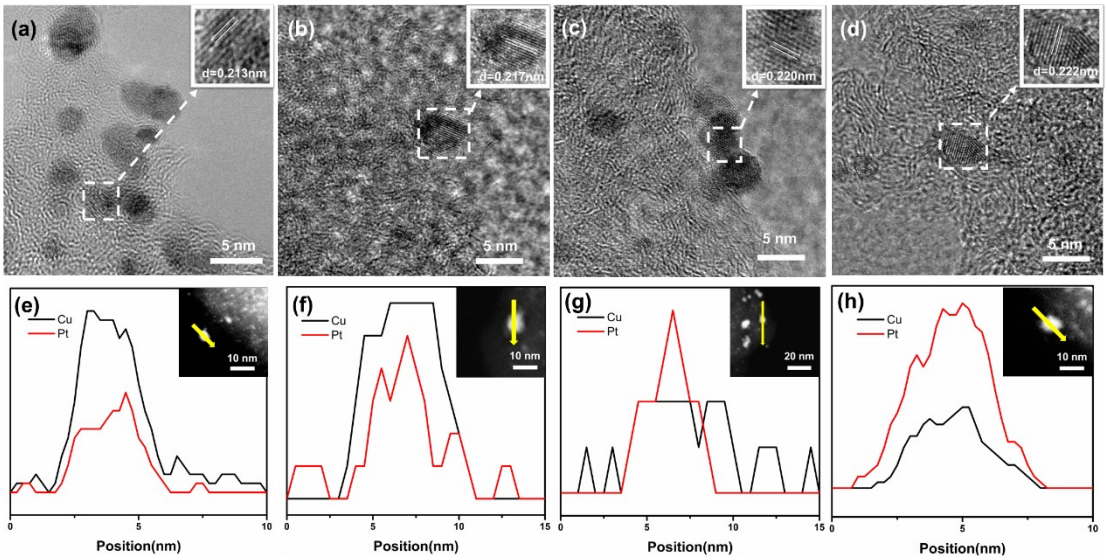

Figure S3. HR-TEM images and corresponding EDS line mapping profiles of (a,e) Pt-Cu_4/AC; (b,f) Pt-Cu_2/AC; (c,g) Pt_2-Cu/AC and (d,h)Pt_4-Cu/AC.

Figure S3 presents the HR-TEM images of Pt-Cu_4/AC, Pt-Cu_2/AC, Pt_2-Cu/AC and Pt_4-Cu/AC catalysts. The Pt-Cu nanocrystals display well-defined lattice fringes with the lattice spacing of 0.213-0.222 nm (Fig. S3a-d), which is slightly smaller than the d-spacing of cubic Pt (111) (0.226 nm) and larger than that of cubic Cu (111) (0.209 nm). These results demonstrate that these supported Pt-Cu nanocrystals existed in the alloyed state, and the variation of lattice spacing of Pt-Cu alloy is due to the compression of Pt crystals cells caused by the addition of Cu. Moreover, the composition distributions are uniform for the studied nanoparticle according to the EDS line mapping profiles (Fig. S3e-h).

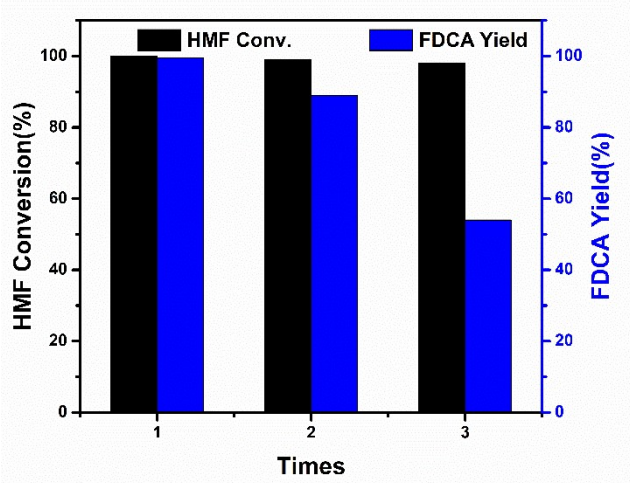

Figure S4. Recycling test over Pt-$Cu_{1.5}$/C. Reaction conditions: 0.3mmol of HMF, 40mg catalyst, 4 mL of H_2O, 1 MPa of O_2, 150°C / 6h.

As displayed in Figure S5, the recyclability of Pt-$Cu_{1.5}$/AC catalyst has been tested, and the conversion of HMF did not show a noticeable decrease accompany with moderate decrease in the FDCA yield after the second reuse. According to the ICP analysis of the reused catalyst, the loading of Pt and Cu were 0.44 wt.% and 0.15 wt.%, respectively. Compared with the fresh catalyst, the slightly loss of Cu species resulted in the decrease of FDCA yield.

Table S1. A comparative table with the reported catalytic systems for the oxidation of HMF to FDCA.

Entry	Catalyst	Solvent	$P(O_2)$ [MPa]	Base/Additive	T (ºC)	Time (h)	HMF Conversion [%]	FDCA Selectivity [%]	TON or TOF(h^{-1})	Ref.
				Heterogeneous catalysts						
1	Pt-Cu/AC	H_2O	1.0	-	150	6	100	99	135	This work
2	Pt-PVP-GLY	H_2O	0.1	-	80	24	99	99	2.8	1
3	Pt@Dowex-Na	H_2O	2	-	120	22	100	98	14.4	2
4	Pt/C–O–Mg	H_2O	1	-	110	12	>99	97	20	3
5	Pt/Ni_{25a}	H_2O	1	-	100	12	100	100	22.2	4
6	$Pt/NC\text{-}CeO_2$	H_2O	0.4	-	150	4	100	99.9	114	5
7	Pt/PVP-ACS-800	H_2O	1	-	110	5	>99	>99	21.5	6
8	Pt−Ni/AC-15ALD	H_2O	0.8	-	100	15	>99	98	24.3	7
9	Au/MgO	H_2O	2.6	-	110	2	99	91	25	8
10	Au/HT	H_2O	0.1	-	95	7	>99	>99	32	9
11	Au-Pd/MgO	H_2O	0.5	-	100	12	100	99	80	10
12	AuPd/La-CaMgAl-LDH	H_2O	0.5	-	100	6	96.1	89.4	6.4	11
13	AuPd-nNiO	H_2O	1	-	90	6	95	70	19.5	12
14	$Ru/ZrO_{2\ H\text{-}aero}$	H_2O	1	-	120	16	100	97	10.9	13
15	$Ru/Mn_6Ce_1O_Y$	H_2O	1	-	150	15	100	>99	15	14
16	Ru/CTF	H_2O	2	-	140	3	99	77.6	40	15
17	Co-N-C-9.6	H_2O	1.0	$NaHCO_3$	120	1	>99	94.3	477	16
18	$Ru\text{-}Fe_3O_4@SiO_2$	H_2O	1.0	n-butylamine	110	48	92	80.6	2.4	17
19	$Pd\text{-}MnO_2$	H_2O	0.1	K_2CO_3	100	4	100	88.1	151.2	18

20	Pd@Beta	H_2O	0.1	Na_2CO_3	90	24	99	98	451	19
21	Pd/HPGS	H_2O	0.1	NaOH	50	5	99	82	62	20
22	Pd/C@Fe_3O_4	H_2O	30 mL min^{-1}	K_2CO_3	80	6	98.4	86.7	4.5	21
23	γ-Fe_2O_3@HAP-Pd(0)	H_2O	30 mL min^{-1}	K_2CO_3	100	6	97	92.9	3.09	22
24	C–Fe_3O_4–Pd	H_2O	30 mL min^{-1}	K_2CO_3	80	4	98.2	91.8	13.4	23
25	Pd/C@Fe_3O_4	H_2O	30 mL min^{-1}	K_2CO_3	80	6	100	87.8	4.6	24
26	$Ni_{0.90}Pd_{0.10}$	H_2O	air bubbling	Na_2CO_3	80			70	35	25
27	Pt-NCs	H_2O	75 mL min^{-1}	$NaHCO_3$	100	10	100	95.1	391.8	26
28	Au/TiO_2	H_2O	2	NaOH	25	22	100	79	4.5	27
29	Pt_{imp}-Bi/C_{3SW}	H_2O	4	Na_2CO_3	100	3	>99	99	16.7	28
30	Pt-Bi/TiO_2	H_2O	4	Na_2CO_3	100	10	>99	>99	9.9	29
31	CoO_x-MC	H_2O	0.5	K_2CO_3	80	30	98.3	95.3	2.22	30
32	$AuCe_{25}Zr$	H_2O	1	NaOH	70	4	>99	85	17.5	31
33	Au/HT	H_2O	10 $ml.min^{-1}$	NaOH	90	7	>99	89	11.2	32
34	Au/TiO_2	H_2O	2	NaOH	30	18	>99	71	5.6	33
35	Au/ZrO_2	H_2O	1	NaOH	125	5	>99	89	67	34
36	Au/HT	H_2O	0.1	Na_2CO_3	95	7	99	99	1.4	35
37	Au_1-Pd_1@PECN	H_2O	10 mL min^{-1}	K_2CO_3	90	12	99.7	99	36.3	36
38	Au_1Pd_3/pBN_2C-800	H_2O	3	Na_2CO_3	100	24	100	97.6	29	37
39	Au_8-Pd_2/AC	H_2O	0.3	NaOH	60	2	>99	99	100	38
40	Au/MZ-600	H_2O	50 mL min^{-1}	NaOH	95	4	100	95	71	39
41	Au/HSAG-N	H_2O	1	$NaHCO_3$	90	12	>99	75	1195	40
42	Au–Cu/TiO_2	H_2O	1	NaOH	95	4	>99	99	120	41
43	Au_2O_3/Ag_2O/$Cu(NO_3)_2 \cdot 3H_2O$	H_2O	0.1	NaOH	42	16	99	93	2.37	42
44	Ru/C	H_2O	0.2	Na_2CO_3	120	5	100	93	45	43
45	M400(Mn_2O_3)	H_2O	1.4	$NaHCO_3$	100	24	>99	99.5	1.05	44

46	$CuMn_2O_4$	H_2O	1	$NaHCO_3$	120	18	100	92.1	0.05	45
47	Mn_2O_3	H_2O	1	$NaHCO_3$	100	24	>99	91	0.91	46
48	MnO_2	H_2O	1	$NaHCO_3$	100	24	>99	74	0.014	47
				Homogeneous catalysts						
49	Co/Mn/Br	H_2O/HOAc	CO_2/O_2 = 1/1 6MPa	-	180	0.5	>99	78.8	5.9	48

TOF value was calculated according to the equation below:

$$TOF = \frac{Convention\ of\ HMF(mol)}{Metal\ loading\ on\ the\ catalyst\ surface(mol) * Reaction}$$

Supplementary References:

1. S. Siankevich, G. Savoglidis, Z. Fei, G. Laurenczy, D. T. L. Alexander, N. Yan and P. J. Dyson, *J. Catal.*, 2014, **315**, 67–74.
2. F. Liguori, P. Barbaro and N. Calisi, *ChemSusChem*, 2019, **12**, 2558 – 2563.
3. X. Han, L. Geng, Y. Guo, R. Jia, X. Liu, Y. Zhang and Y. Wang, *Green Chem.*, 2016, **18**, 1597–1604.
4. H. Zhang, T. Gao, Q. Cao and W. Fang, *ACS Sustainable Chem. & Eng.,* 2021, **9**, 6056-6067.
5. C. Ke, M. Li, G. Fan, L. Yang and F. Li, *Chemistry*, 2018, **13**, 2714-2722.
6. H. Yu, K.-A. Kim, M. J. Kang, S. Y. Hwang and H. G. Cha, *ACS Sustainable Chem. Eng.*, 2019, **7**, 3742−3748.
7. J. Shen, H. Chen, K. Chen, Y. Qin, X. Lu, P. Ouyang and J. Fu, *Ind. Eng. Chem. Res.*, 2018, **57**, 2811−2818.
8. C. P. Ferraz, M. Zieliński, M. Pietrowski, S. Heyte, F. Dumeignil, L. M. Rossi and R. Wojcieszak, *ACS Sustainable Chem. & Eng.*, 2018, **6**, 16332-16340.
9. N. K. Gupta, S. Nishimura, A. Takagakib and K. Ebitani, *Green Chem.*, 2011, **13**, 824–827.
10. X. Wan, C. Zhou, J. Chen, W. Deng, Q. Zhang, Y. Yang and Y. Wang, *ACS Catal.*, 2014, **4**, 2175-2185.
11. Z. Gao, R. Xie, G. Fan, L. Yang and F. Li, *ACS Sustainable Chem. Eng.*, 2017, **5**, 5852−5861.
12. D. Bonincontro, A. Lolli, A. Villa, L. Prati, N. Dimitratos, G. M. Veith, L. E. Chinchilla, G. A. Botton, F. Cavani and S. Albonetti, *Green Chem.*, 2019, **21**, 4090–4099.
13. C. M. Pichler, M. G. Al-Shaal, D. Gu, H. Joshi, W. Ciptonugroho and F. Schuth, *ChemSusChem*, 2018, **11**, 2083-2090.
14. T. Gao, J. Chen, W. Fang, Q. Cao, W. Su and F. Dumeignil, *J. Catal.,* 2018, **368**, 53–68.
15. J. Artz and R. Palkovits, *ChemSusChem*, 2015, **8**, 3832 – 3838.
16. X. Liu , Y. Luo, H. Ma, S. Zhang, P. Che, M. Zhang, J. Gao and J. Xu, *Angew. Chem. Int. Ed.*, 2021, **60**, 2-10.
17. A. Tirsoaga, E. M. Fergani, I. V. Parvulescu and M. S. Coman, *ACS Sustainable Chem. Eng.*, 2018, **6**, 14292−14301.
18. X. Liao, J. Hou, Y. Wang, H. Zhang, Y. Sun, X. Li, S. Tang, K. Kato, Y. Miho and Z. Jiang, *Green Chem.*, 2019, **21**, 4194–4203.
19. W. Zhuang, X. Liu, L. Chen, P. Liu, H. Wen, Y. Zhou and J. Wang, *Green Chem.*, 2020, **22**, 4199–4209.
20. C. Chen, X. Li, L. Wang, T. Liang, L. Wang, Y. Zhang and J. Zhang, *ACS Sustainable Chem. &*

Eng., 2017, **5**, 11300-11306.
21. B. Liu, Y. Ren and Z. Zhang, *Green Chem.*, 2015, **17**, 1610–1617.
22. Z. Zhang, J. Zhen, B. Liu, K. Lv and K. Deng, *Green Chem*., 2015, **17**, 1308–1317.
23. N. Mei, B. Liu, J. Zheng, K. Lv, D. Tang and Z. Zhang, *Catal. Sci. Technol.*, 2015, **5**, 3194-3203.
24. B. Liu, Y. Ren and Z. Zhang, *Green Chem.*, 2015, **17**, 1610-1618.
25. K. Gupt, R. K. Rai, A. D. Dwivedi and S. K. Singh, *ChemCatChem*, 2017, **9**, 2760-2767.
26. Y. Liu, H.-Y. Ma, D. Lei, L.-L. Lou, S. Liu, W. Zhou, G.-C. Wang and K. Yu, *ACS Catal.*, 2019, **9**, 8306−8315.
27. S. E. Davis, B. N. Zope and R. J. Davis, *Green Chem.*, 2012, **14**, 143-147.
28. H. A. Rass, N. Essayem and M. Besson, *Green Chem.*, 2013, **15**, 2240–2251.
29. H. Ait Rass, N. Essayem and M. Besson, *ChemSusChem*, 2015, **8**, 1206-1217.
30. X. Liu, M. Zhang and Z. Li, *ACS Sustainable Chem. Eng.*, 2020, **8**, 4801−4808.
31. C. Megías-Sayago, K. Chakarova, A. Penkova, A. Lolli, S. Ivanova, S. Albonetti, F. Cavani and J. A. Odriozola, *ACS Catal.*, 2018, **8**, 11154−11164.
32. L. Ardemani, G. Cibin, A. J. Dent, M. A. Isaacs, G. Kyriakou, A. F. Lee, C. M. A. Parlett, S. A. Parry and K. Wilson, *Chem. Sci.*, 2015, **6**, 4940–4945.
33. Y. Y. Gorbanev, S. K. Klitgaard, J. M. Woodley, C. H. Christensen and A. Riisager, *ChemSusChem*, 2009, **2**, 672 – 675.
34. O. R. Schade, K. F. Kalz, D. Neukum, W. Kleist and J.-D. Grunwaldt, *Green Chem.*, 2018, **20**, 3530–3541.
35. G. Yi, S. P. Teong, X. Li and Y. Zhang, *ChemSusChem*, 2014, **7**, 2131 – 2137.
36. Q. Wang, W. Hou, S. Li, J. Xie, J. Li, Y. Zhou and J. Wang, *Green Chem.*, 2017, **19**, 3820-3830.
37. W. Guan, Y. Zhang, Y. Chen, J. Wu, Y. Cao, Y. Wei and P. Huo, *J. Catal.*, 2021, **396**, 40-53.
38. A. Villa, M. Schiavoni, S. Campisi, G. M. Veith and L. Prati, *ChemSusChem*, 2013, **6**, 609 – 612.
39. A. Rabee, S. D. Le, K. Higashimine and S. Nishimura, *ACS Sustainable Chem. Eng.*, 2020, **8**, 7150–7161.
40. B. Donoeva, N. Masoud and P. E. d. Jongh, *ACS Catal.*, 2017, **7**, 4581−4591.
41. T. Pasini, M. Piccinini, M. Blosi, R. Bonelli, S. Albonetti, N. Dimitratos, J. A. Lopez-Sanchez, M. Sankar, Q. He, C. J. Kiely, G. J. Hutchings and F. Cavania, *Green Chem.*, 2011, **13**, 2091-2099.
42. Y. Yamamoto, M. Ota, S. Kodama, K. Michimoto, A. Nomoto, A. Ogawa, M. Furuya and K. Kawakami, *ACS Omega*, 2021, **6**, 2239−2247.
43. G. Yi, S. P. Teong and Y. Zhang, *Green Chem.*, 2016, **18**, 979–983.
44. L. Bao, F.-Z. Sun, G.-Y. Zhang and T.-L. Hu, *ChemSusChem*, 2019, **13**, 548-555.
45. X. Wan, N. Tang, Q. Xie, S. Zhao, C. Zhou, Y. Dai and Y. Yang, *Catal. Sci. Technol.*, 2021, **11**, 1497-1509
46. E. Hayashi, T. Komanoya, K. Kamata and M. Hara, *ChemSusChem*, 2016, **10**, 654-658.
47. E. Hayashi, Y. Yamaguchi, K. Kamata, N. Tsunoda, Y. Kumagai, F. Oba and M. Hara, *J. Am. Chem. Soc.*, 2019, **141**, 890−900.

48. X. Zuo, P. Venkitasubramanian, D. H. Busch and B. Subramaniam, *ACS Sustainable Chem. Eng.*, 2016, **4**, 3659−3668.